Enhancement-Mode Pseudomorphic Inverted HEMT for Low Noise Amplifier

Kazuhiko Ohmuro, Hiroki Inomata Fujishiro, Masaaki Itoh, Hiroshi Nakamura, and Seiji Nishi

Abstract—**Characteristics of pseudomorphic inverted HEMT (P-I-HEMT) are compared with that of pseudomorphic HEMT. Both devices were fabricated in enhancement-mode by the same process. P-I-HEMT shows higher maximum transconductance of 590 mS/mm, and higher K-value of 600 mS/Vmm at threshold voltage of 0 V, and good pinch-off characteristics than its counterpart. Noise characteristics of P-I-HEMT are reported for the first time in this paper. Lower noise figure (1.0 dB at 18 GHz) was obtained in P-I-HEMT. It is concluded that the P-I-HEMT structure is suitable for fine gate low noise FET's. Furthermore, P-I-HEMT shows far better noise characteristics than the other at low drain voltage and current.**

Introduction

HEMT structures, especially pseudomorphic HEMT (P-HEMT) structures are used for low noise FET devices due to their high electron mobility and good carrier confinement [1]–[3]. A layer structure suppressing short channel effects with superior carrier confinement is thought to be very advantageous to fine gate low noise devices. In this respect, inverted HEMT structure, which has a GaAs layer located on an AlGaAs, is a prime candidate of low noise fine gate devices [4]. To maximize the merits of inverted HEMT, improving transconductance (g_m) by increasing two-dimensional electron gas (2DEG) concentration and/or by shortening the gate to channel distance are essential.

In order to increase the 2DEG concentration, InGaAs strained layer was inserted into the hetero-interface of inverted HEMT to make its energy band gap larger. This structure is called pseudomorphic inverted HEMT (P-I-HEMT) [5]. To shorten the gate to channel distance, P-I-HEMT is used in enhancement-mode (with positive threshold voltage). In this P-I-HEMT, our simulation study shows excellent carrier confinement and suppression of short channel effects, so it is expected to have an improved noise property.

In this paper, the microwave and noise properties of P-I-HEMT's are studied for the first time, and it is observed that the P-I-HEMT is suitable for a low noise device. Its characteristics are compared with that of the P-HEMT fabricated by the same process.

Manuscript received April 10, 1991; revised July 29, 1991.

The authors are with the Semiconductor Technology Laboratory, Oki Electric Industry Co., Ltd., 550-5 Higashiasakawa-cho, Hachioji-shi, Tokyo 193, Japan.

IEEE Log Number 9103293.

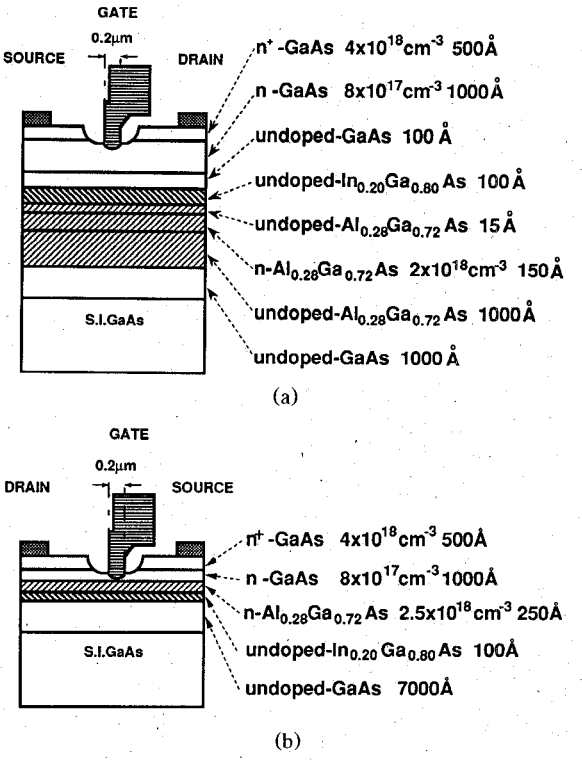

Fig. 1. Schematic cross section of (a) pseudomorphic inverted HEMT and (b) pseudomorphic HEMT.

Fabrication Process

The P-I-HEMT and P-HEMT structures were grown by molecular beam epitaxy. The cross sectional view of the P-HEMT and the P-I-HEMT are indicated in Fig. 1. They have an $In_{0.2}Ga_{0.8}As$ channel of 100 Å thickness. In the P-I-HEMT and the P-HEMT, electron mobilities are almost the same value of 6500 cm^2/Vs at room temperature, and 2DEG concentrations are 1.3×10^{12} cm^{-2} and 1.6×10^{12} cm^{-2} at 77 K, respectively.

The fabrication process of mushroom-shaped fine gate electrode is very unique but simple one, which is illustrated in Fig. 2 [5]. After two layer photoresist was patterned (the aperture of the upper resist was 0.5 μm), thin

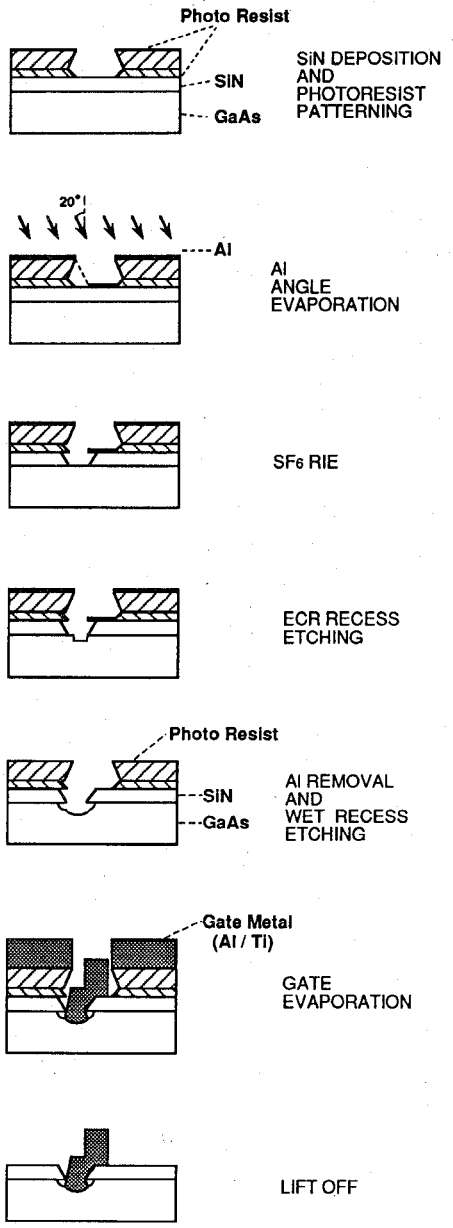

Fig. 2. Fabrication process of 0.2 μm mushroom shaped gate electrode.

Al film was evaporated at a tilted angle of 20°. By this angle evaporation, 0.2 μm slit was formed in Al film on the silicon nitride (SiN), and then SiN film under Al aperture was etched by reactive ion etching to expose GaAs. In enhancement-mode devices, source resistance tends to increase due to the existing space between gate electrode and source n^+ region. To prevent this problem, the stepped recess gate structure was formed using the combination of dry and wet etching [6]. The GaAs was etched anisotropically using electron-cyclotron-resonance-type dry etcher with chlorine gas first, then recess-etched by wet etchant isotropically. Gate metal of Ti/Al was evaporated and lifted off to form the gate cross section as shown in Fig. 3. The 0.2 μm gate electrode was fabricated in the inner recess. The upper part of the gate is wider than the lower part (mushroom-shaped) to reduce gate

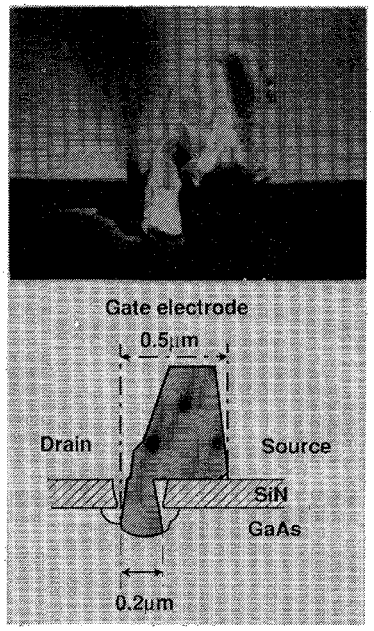

Fig. 3. Cross sectional SEM photograph of 0.2 μm mushroom shaped gate electrode.

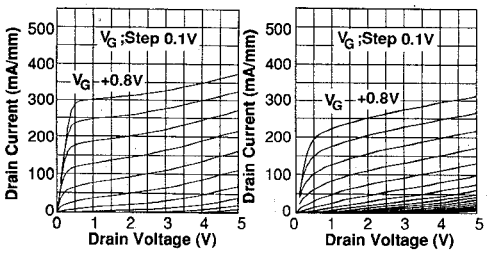

Fig. 4. *I-V* characteristics of (a) pseudomorphic inverted HEMT and (b) pseudomorphic HEMT.

resistance, and the former overhangs to source side not to decrease gain.

DC Characteristics

The *I-V* characteristics of the P-I-HEMT and the P-HEMT are shown in Fig. 4. For both devices, the gate length, width and threshold voltage (V_{th}) are 0.2 μm, 10 μm and approximately 0 V, respectively. The maximum values of transconductance ($g_{m\max}$) of P-I-HEMT and P-HEMT are 590 and 510 mS/mm, respectively. Comparing the pinch-off characteristics in sub-threshold region, the superior performance of the P-I-HEMT to the P-HEMT is observed. Fig. 5 shows the drain conductances ($g_d s$) of P-I-HEMT and P-HEMT as a function of drain voltages. From the figure, g_d of the P-I-HEMT is recognized to be much smaller than that of the P-HEMT. Moreover g_d of the P-I-HEMT maintains low value at small $V_d s$, which comes from the good drain current saturation at small $V_d s$. For example, at a V_d of 2 V and gate voltage (V_g) of 0.5 V, g_d of the P-I-HEMT is 9 mS/mm, whereas that of P-HEMT is 23 mS/mm. From these results, P-I-HEMT has smaller short channel effects

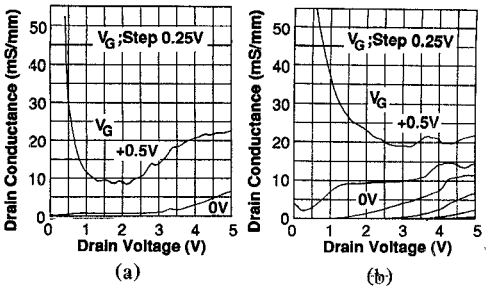

Fig. 5. Drain conductance versus drain voltage of (a) pseudomorphic inverted HEMT and (b) pseudomorphic HEMT.

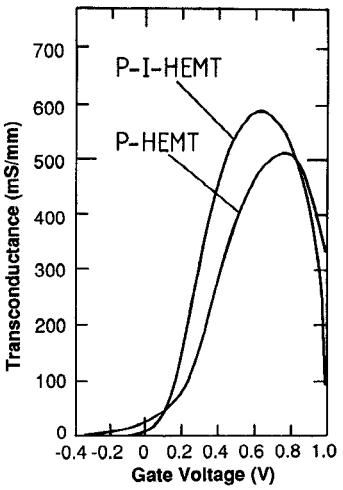

Fig. 6. Transconductances versus gate voltage.

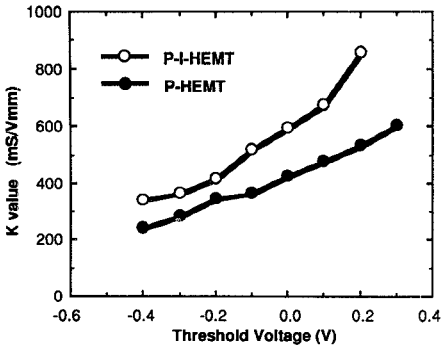

Fig. 7. *K*-value versus threshold voltage.

and thus is a suitable structure for short gate devices, and is advantageous in low drain currents (I_ds). Fig. 6 shows the comparison of g_m curves as a function of V_g for both devices. Better pinch-off characteristics in the P-I-HEMT is also seen from g_m curves in this figure. A steeper rise of g_m with increasing V_g in P-I-HEMT is clearly shown. So the *K*-value (i.e., extracted from $I_d = K(V_g - V_{th})^2$, which represents the g_m in small I_d region) is expected to be higher in P-I-HEMT, too. In Fig. 7, the *K*-value is indicated as a function of V_{th}. As V_{th} becomes more positive, *K*-value of P-I-HEMT increases more sharply than that of P-HEMT. This is because the distance between gate and 2DEG becomes smaller in P-I-HEMT than in P-HEMT as V_{th} goes positive, and that becomes

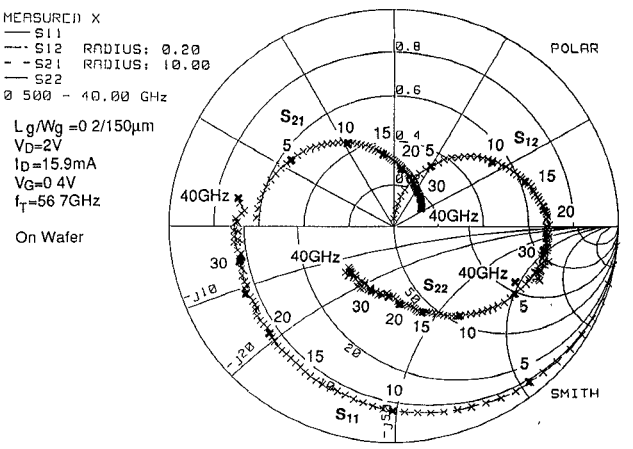

Fig. 8. *S*-parameters of P-I-HEMT.

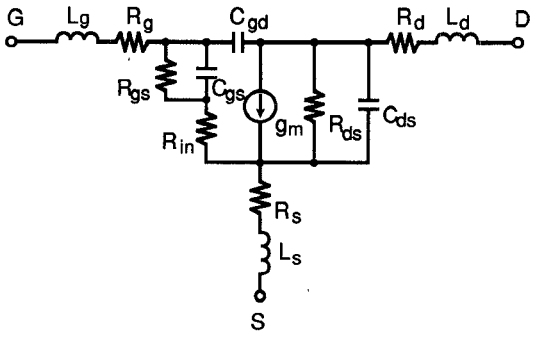

	g_m (mS)	C_{gs} (pF)	R_g (Ω)	R_s (Ω)	R_{in} (Ω)	R_{ds} (Ω)	C_{ds} (fF)	C_{gd} (fF)
P-I-HEMT	78.8	0.19	4.80	0.93	0.59	257	36.5	28.2
P-HEMT	74.4	0.17	4.80	1.15	0.74	186	40.3	26.7

P-I-HEMT; V_{th}=0V, V_d=2V, V_g=0.4V, I_d=15.9mA
P-HEMT ; V_{th}=0V, V_d=2V, V_g=0.5V, I_d=19.0mA

Fig. 9. Equivalent circuit and equivalent circuit constants.

larger as V_{th} goes negative. In the P-I-HEMT and the P-HEMT, *K*-values are 600 mS/Vmm and 430 mS/Vmm at $V_{th} = 0$ V, respectively.

S Parameter Measurements

The on-wafer scattering parameters (*S*-parameters) were measured at frequencies from 0.5 GHz to 40 GHz with 150 μm-wide FET's. The measured S-parameters of P-I-HEMT with $V_{th} = 0$ V, $V_g = 0.4$ V, $I_d = 15.9$ mA, $V_d = 2$ V are shown in Fig. 8. Equivalent circuit constants were extracted from the measured *S*-parameters. The equivalent circuit and some equivalent circuit constants for both devices are shown in Fig. 9. Bias conditions of P-I-HEMT with $V_{th} = 0$ V are the same values noted above, and those of P-HEMT are $V_d = 2$ V, $V_g = 0.5$ V, $I_d = 19.0$ mA. The $g_m/g_d s$ in RF region were 20.3 for P-I-HEMT and 13.8 for P-HEMT, respectively. Although these values are smaller than dc values of 60.3 (P-I-HEMT) and 18.7 (P-HEMT), P-I-HEMT has higher g_m/g_d value than the other and has the ability of high gain.

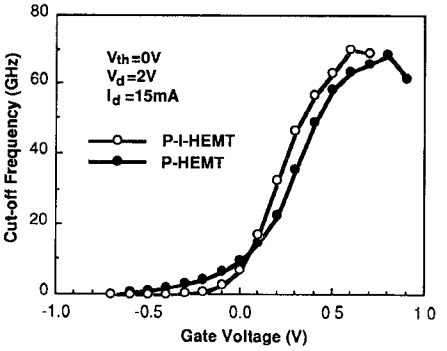

Fig. 10. Cut-off frequency versus gate voltage.

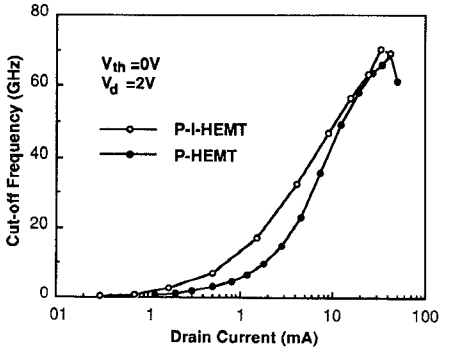

Fig. 11. Cut-off frequency versus drain current in log scale.

The short circuit current gain (h_{21}) was extracted from the S-parameters, and cut-off frequency (f_T) was estimated by extrapolating h_{21} value to unity with a slope of -6 dB/octave. Fig. 10 shows the comparison of f_T versus gate voltage (V_g) in both devices of $V_{\text{th}} = 0$ V. A steeper rise in f_T with increasing V_g was observed in P-I-HEMT. This corresponds to a steeper rise in g_m with increasing V_g as shown in Fig. 6, so to higher K-value in P-I-HEMT. The f_T at $V_g = 0.4$ V is 56.7 GHz for P-I-HEMT and 49.1 GHz for P-HEMT. The maximum f_T is approximately 70 GHz for both devices of $V_{\text{th}} = 0$ V.

Fig. 11 shows the comparison of f_T versus $\log I_d$ in both devices. The f_T at smaller drain currents is higher in the P-I-HEMT, so the P-I-HEMT is expected to have good noise characteristics at small drain currents. For example, f_T at $I_d = 5$ mA is 37 GHz for P-I-HEMT and 26 GHz for P-HEMT. This is due to the good pinch-off characteristic in P-I-HEMT.

In Fig. 12, f_T versus V_g for P-HEMTs and P-I-HEMT's of different V_{th} are plotted. Though f_T peak value is maximum at V_{th} below 0 V in P-HEMT's, f_T peak value increases as V_{th} goes positive in P-I-HEMT's. P-I-HEMT's, therefore, have higher f_T in enhancement-mode than in depletion-mode.

Noise Characteristics

Noise parameter measurements were performed using the noise parameter test set NP4 (by ATN). Measured devices are 150 μm-wide FET with three gate feeds to reduce gate resistance. The frequency dependence of minimum noise figures (F_{min}) and associated gains (G_{as})

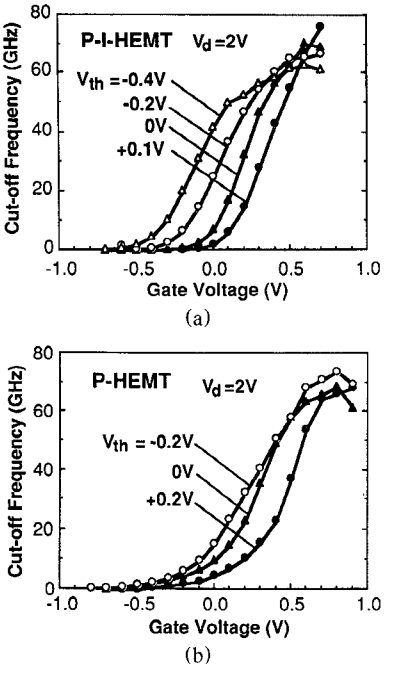

Fig. 12. Cut-off frequency versus gate voltage for (a) pseudomorphic inverted HEMT and (b) pseudomorphic HEMT of different threshold voltages.

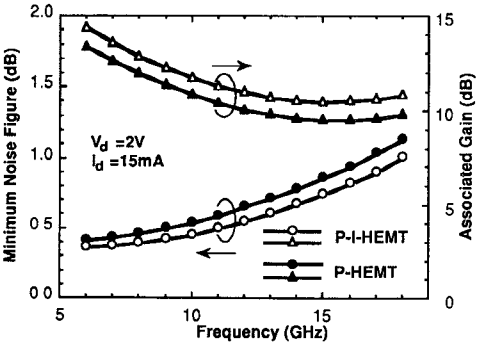

Fig. 13. Minimum noise figures and associated gains versus frequency.

at $I_d = 15$ mA, $V_d = 2$ V for P-HEMT and P-I-HEMT are shown in Fig. 13. F_{min} are about 0.1 dB smaller and the G_{as} are 1 dB larger for the P-I-HEMT than for the P-HEMT in the frequency range from 6 GHz to 18 GHz. The F_{min} at 12 GHz and 18 GHz are 0.56 dB (G_{as} 11.0 dB) and 1.01 dB (G_{as} 10.9 dB) for the P-I-HEMT, and 0.66 dB (G_{as} 10.1 dB) and 1.14 dB (G_{as} 9.9 dB) for the P-HEMT.

At small drain voltages, P-I-HEMT's have superior characteristics than P-HEMT's, because the former shows good current saturation at low drain voltages as shown in Fig. 4. Fig. 14 shows F_{min} and G_{as} versus V_d at 12 GHz and $I_d = 15$ mA. In V_d region smaller than 1 V, degradation of noise characteristics is not so fierce in the P-I-HEMT as in the P-HEMT. F_{min} at 0.6 V and 0.4 V are 0.66 dB and 1.01 dB for the P-I-HEMT, and are 0.98 dB and 2.71 dB for the P-HEMT, respectively. These lower F_{min} in small V_d region for the P-I-HEMT are thought to be due to early drain current saturation and small g_d in this region. Lower F_{min} is obtained for the P-I-HEMT

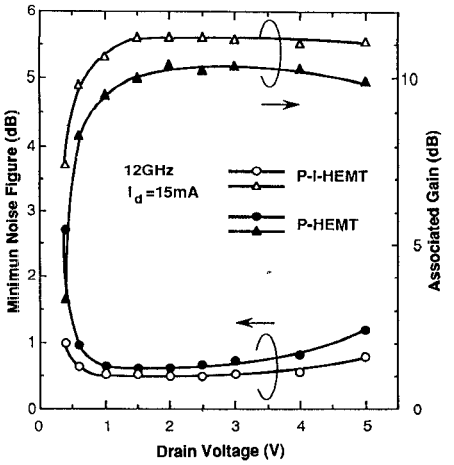

Fig. 14. Minimum noise figures and associated gains versus drain voltage.

TABLE I
TYPICAL PERFORMANCE DATA OF P-I-HEMT AND P-HEMT

	P-I-HEMT	P-HEMT
Current Pinch-Off	Good	Poor
g_d in dc (V_d = 2 V, V_g = 0.5 V)	9 mS/mm	23 mS/mm
$g_{m\max}$ (V_d = 2 V)	590 mS/mm	510 mS/mm
K-value	600 mS/Vmm	430 mS/Vmm
g_m/g_d in RF*	20.3	13.8
$f_{T\max}$ (V_d = 2 V)*	70 GHz	69 GHz
f_T (V_d = 2 V, I_d = 5 mA)*	37 GHz	26 GHz
$F_{\min}$ V_d = 2 V, I_d = 15 mA*	0.56 dB	0.66 dB
(12 GHz) V_d = 0.6 V, I_d = 15 mA*	0.66 dB	0.98 dB
V_d = 2 V, I_d = 5 mA*	0.58 dB	1.18 dB
P_{out} (−1 dB) at 12 GHz* V_d = 2 V, I_d = 15 mA	5.5 dBm	3.5 dBm

*W_g = 150 μm
L_g = 0.2 μm, V_{th} = 0 V (enhancement-mode)

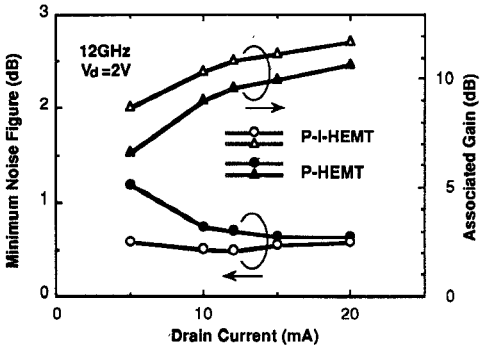

Fig. 15. Minimum noise figures and associated gains versus drain current.

than its counterpart also in the V_d region from 1 V to 4 V. In this region, P-I-HEMT's have better pinch-off characteristics than P-HEMT's.

At small drain currents, P-I-HEMT's have superior characteristics than P-HEMT's, because of the good pinch-off characteristics in this region. Fig. 15 shows $F_{\min}$ and G_{as} versus I_d at 12 GHz and V_d = 2 V. Little degradation of $F_{\min}$ is seen down to I_d = 5 mA in the P-I-HEMT, whereas $F_{\min}$ of the P-HEMT degrades at small I_d. At I_d = 5 mA, $F_{\min}$ are 0.58 dB (G_{as} 8.78 dB) for P-I-HEMT and 1.18 dB (G_{as} 6.68 dB) for P-HEMT. So the P-I-HEMT is proved to be useful in small drain currents. Moreover, the P-I-HEMT maintains low $F_{\min}$ in I_d region from 5 mA to 20 mA, so it can be used with a wide margin about drain current.

From these results, enhancement-mode P-I-HEMT's show better noise characteristics at small drain currents and for small drain voltages than P-HEMT's, so they are advantageous for low noise devices with low power consumption. There is still room to make a much lower $F_{\min}$ by reducing C_{gs}. Here, C_{gs} has become high owing to the rather large overhang of the gate electrode and to the large dielectric constant of SiN under the overhang. When C_{gs} is reduced by narrowing the upper part of the gate electrode and by eliminating the SiN under that, noise characteristics could be improved.

Noise characteristics of P-I-HEMT's, as they do not show the obvious short channel effects even at this gate length, are expected to be further improved by adopting it to devices of under 0.2 μm gate length. In addition, the use of enhancement-mode low noise FET will have the merit of simplifying the power supply circuit, especially in the MMIC's.

For low noise applications, such as a head amplifier, the device must have a certain amount of output power to avoid intermoduration problem, which might be considered to be uneasy in enhancement-mode operation. Then the output power was measured at 12 GHz, I_d = 15 mA and V_d = 2 V. The measured 1 dB compression power was 5.5 dBm for P-I-HEMT and 3.5 dBm for P-HEMT. These are sufficiently high values to be used in a conventional low noise application.

CONCLUSION

Enhancement-mode pseudomorphic inverted HEMT's (P-I-HEMT's) were fabricated and the properties were compared with pseudomorphic HEMT's (P-HEMT's). Dry/wet recess etching process and mushroom-shaped gate electrode was adopted to reduce source and gate resistance, respectively.

The typical performance data were indicated in Table I. In DC characteristics of enhancement-mode FET, the P-I-HEMT has better pinch-off property, smaller g_d, and higher g_m and K-value than its counterpart. At V_{th} = 0 V, obtained g_d, $g_{m\max}$ and K-value are 9 mS/mm (V_g = 0.5 V), 590 mS/mm and 600 mS/Vmm in P-I-HEMT, and 23 mS/mm (V_g = 0.5 V), 510 mS/mm and 430 mS/Vmm in P-HEMT.

From S-parameter measurements, equivalent circuit elements and cut-off frequency were extracted. The g_m/g_d value is 20.3 in P-I-HEMT, that is higher than the value 13.8 in P-HEMT. The P-I-HEMT has steeper increase of

f_T with V_d, and has a higher value of f_T at low drain currents. The maximum f_T is approximately 70 GHz for both devices. Though f_T peak value is maximum at V_{th} below 0 V in P-HEMT, f_T peak value increases as V_{th} goes positive in P-I-HEMT. Hence the P-I-HEMT is more effective in enhancement-mode.

In the noise measurement, the P-I-HEMT exhibits a minimum noise figure 0.1 dB lower and an associated gain 1 dB higher than the other in the frequency range from 6 GHz to 18 GHz. F_{min} and G_{as} at 12 GHz are 0.56 dB and 11.0 dB. In P-I-HEMT, little noise degradation are seen both in wider drain voltage region from below 1 V to 4 V and in wider drain current region from 5 mA to 20 mA. P-I-HEMT can be used with a wide margin about drain voltage and drain current. Moreover, it has far better noise characteristics even at small V_d and I_d, and hence has the capability of realizing low noise devices with low power consumption. Noise characteristics of P-I-HEMT are expected to be further improved by adopting it to devices of under 0.2 μm gate length.

Acknowledgment

The authors would like to acknowledge M. Sakuta and S. Takahashi for their encouragement during this work. We are also grateful to S. Kuribayashi and R. Komatsu for noise measurements.

References

[1] K. H. G. Duh *et al.*, "Millimeter-wave low-noise HEMT amplifiers," in *1988 IEEE MTT-S Int. Microwave Symp. Dig.*, 1988, pp. 923–926.
[2] P. C. Chao *et al.*, "0.1 μm gate-length pseudomorphic HEMT's," *IEEE Electron Device Lett.*, vol. EDL-8, pp. 489–491, Oct. 1987.
[3] M. Itoh *et al.*, "Effect of InGaAs well width on low-noise performance in AlGaAs/InGaAs pseudomorphic HEMT," in *Extended Abstracts 21st Conf. Solid State Devices and Materials Rec.*, Tokyo, Japan, 1989, pp. 285–288.
[4] S. Nishi *et al.*, "High performance inverted HEMT and its application to LSI," *Inst. Phys. Conf. Ser.*, no. 83, *Int. Symp. GaAs and Related Compounds Rec.*, pp. 515–520, 1986.
[5] H. I. Fujishiro *et al.*, "0.2 μm gate pseudomorphic InGaAs/AlGaAs inverted HEMT's," *Int. Symp. GaAs and Related Compounds*, Inst. Phys. Conf. Ser. no. 112, ch. 7, 1990, pp. 453–458.
[6] H. Tsuji *et al.*, "A sub-10 ps/gate direct-coupled FET logic circuit with 0.2 μm-gate GaAs MESFET," *Japanese Journal of Applied Physics*, vol. 29, no. 12, Dec., 1990, pp. L2438–L2441.

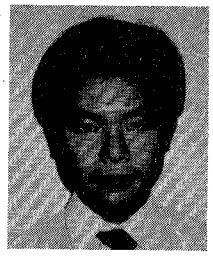

Kazuhiko Ohmuro was born in Saitama, Japan on February 18, 1961. He received the B.S. from Saitama University, Urawa, Japan, in 1984, and M.S. from Kanazawa University, Kanazawa, Japan, in 1986.

He then joined the Research Laboratory, Oki Electric Industry, Tokyo, where he is currently engaged in research and development of GaAs FET for microwave low noise devices.

Mr. Ohmuro is a member of the Japan Society of Applied Physics and the Institute of Electronics, Information and Communication Engineers of Japan.

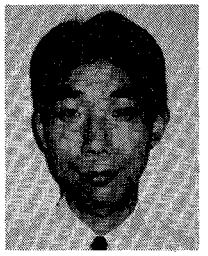

Hiroki Inomata Fujishiro was born in Kanagawa, Japan, on September 30, 1959. He received the B.S. and M.S. degrees in physics from the Science University of Tokyo, Tokyo, Japan, in 1982 and 1984, respectively.

In 1984, he joined the Research Laboratory, Oki Electric Industry Company, Ltd., Tokyo, where he has been engaged in the research and development of MBE growth of compound semiconductors and device technology for heterostructure FET's.

Mr. Fujishiro is a member of the Japan Society of Applied Physics.

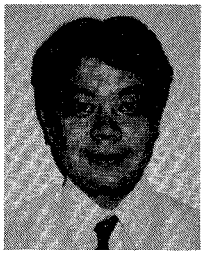

Masaaki Itoh was born in Gifu, Japan, on February 9, 1958. He received the B.S. and M.S. degrees in electronic engineering from Nagoya Institute of Technology, Nagoya, Japan, in 1981, and 1983, respectively.

In 1983, he joined the Research Laboratory, Oki Electric Industry Company, Ltd., Tokyo. He is currently engaged in research and development of MBE growth and HEMT devices.

Mr. Itoh is a member of the Japan Society of Applied Physics, and the Institute of Electronics, Information and Communication Engineers of Japan.

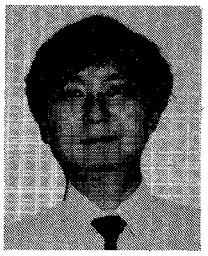

Hiroshi Nakamura was born in Fukuoka, Japan on Oct. 13, 1954. He received the B.E., M.E., and Ph.D. degrees in electronic engineering from the University of Tokyo, Japan, in 1977, 1979, and 1982, respectively.

He then joined Oki Electric Industry Co., Ltd., Tokyo, Japan. He is currently engaged in the microwave GaAs IC technologies.

Dr. Nakamura is a member of the Japan Society of Applied Physics and the Institute of Electronics, Information and Communication Engineers of Japan.

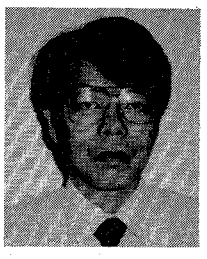

Seiji Nishi was born in Kanagawa, Japan, on April 18, 1950. He received the B.S., M.S. and Ph.D. degrees in physics from Osaka University, Osaka, Japan, in 1974, 1976, and 1979, respectively.

In 1979, he joined the Research Laboratory, Oki Electric Industry Company, Ltd., Tokyo. He is currently engaged in research and development of MBE growth and HEMT devices.

Dr. Nishi is a member of the Japan Society of Applied Physics, and the Institute of Electronics, Information and Communication Engineers of Japan.